Available online at www.sciencedirect.com
SCIENCE DIRECT®
PERGAMON
Electrochimica Acta 48 (2003) 1567–1571
ELECTROCHIMICA Acta
www.elsevier.com/locate/electacta

Effect of oxygenation on electrocatalysis of $La_{0.6}Ca_{0.4}CoO_{3-x}$ in bifunctional air electrode

Nae-Lih Wu *, Wei-Ren Liu, Sern-Jei Su

Department of Chemical Engineering, National Taiwan University, Taipei 106, Taiwan, People's Republic of China

Received 11 November 2002; received in revised form 10 January 2003

Abstract

A vacuum-annealed $La_{0.6}Ca_{0.4}CoO_{3-x}$ was consecutively oxygenated in air at temperatures decreasing from 800 to 100 °C, and its electrocatalytic activities for oxygen reduction and evolution were then measured as a function of the oxygenation temperature. The valence of Co cation, changing between +2 and +3, was found susceptible to annealing either in vacuum or air. The catalytic activities initially decrease monotonically as the oxygenation temperature was decreased from 800 to 300 °C, as a result of increasing oxygen content, and then rise abruptly with the oxygen reduction activity reaching a maximum at 200 °C and the oxidation activity at 150 °C. X-ray photoelectron spectroscopy analysis indicated that the enhancements by the low-temperature oxygenation involved increased OH coverage and less charged cations at surface. The results clearly reveal the importance of the post-calcination annealing process for optimizing the performance of $La_{0.6}Ca_{0.4}CoO_{3-x}$ in air electrode applications.

Keywords: Zinc–air battery; Perovskite oxide; Air electrode; Cathodic catalyst; Oxygen vacancy

1. Introduction

Calcium-doped perovskite $LaCoO_3$, particularly $La_{0.6}Ca_{0.4}CoO_{3-x}$, has drawn considerable attention for bifunctional air electrode applications [1–6]. When added as a catalyst to the carbon air electrode, the oxide catalyst helped to reduce the over-voltage for both oxygen reduction and evolution (oxidation). The electrocatalytic activity has been shown to depend heavily on the nature of synthesis technique as well as the exact conditions employed. In this regard, several previous studies [3–5] have tried to correlate the catalytic performance with microstructural properties such as surface area and pore size distribution. Nevertheless, another structural issue at a much finer scale, namely the issue of oxygen vacancy, associated with processing has not been adequately addressed. Indeed, oxygen vacancy is well known [7–9] to play a very important role in affecting the physical properties, such as lattice stability, ionic conductivity, and electronic superconductivity, of perovskite oxides akin to the present one. In general, the density of oxygen vacancy in these oxides can be varied via, at least, two approaches. The first approach is by doping of the A-site cation (i.e., La^{3+}) with other cations having different valences, such as in the case of $La_{1-y}M_yCoO_{3-z}$, where M is either Ca or Sr [2,10]. Even with a fixed doping level, the amount of oxygen vacancy can also be varied to some extent by moving oxygen into and out of the lattice by thermal annealing under oxidizing and reducing atmospheres, respectively [7–9]. It is this approach that makes the oxygen vacancy strongly affected by the annealing process adopted following the high-temperature calcination step. Nevertheless, the post-calcination annealing process has neither been well characterized nor optimized in previous works except in one case, where Lee et al. [3] noticed significant differences in electrocatalytic activity of $La_{0.6}Ca_{0.4}CoO_{3-x}$ caused by varied cooling rates in an oxidizing atmosphere. They attributed such differences to variations in specific surface area, but, according to their data, the activity was apparently not in proportion to the specific surface areas of the powders. In addition, their data also indicated that the

* Corresponding author.
E-mail address: nlw001@ccms.ntu.edu.tw (N.-L. Wu).

0013-4686/03/$ - see front matter
doi:10.1016/S0013-4686(03)00033-1

activities toward oxygen evolution and reduction were affected differently by cooling rate.

It is the object of this study to access the significance of the post-calcination annealing treatment on the electrocatalytic activity of $La_{0.6}Ca_{0.4}CoO_{3-x}$. One of the issues of focus is the effect of oxygen content. The study was carried out by continuously "pumping" more and more oxygen into the lattice of an originally oxygen-deficient $La_{0.6}Ca_{0.4}CoO_{3-x}$ powder at consecutively decreasing temperatures, and the electrocatalytic activity of the oxide was measured as a function of the oxygenation temperature. In this case, the effect due to oxygen vacancy can be better understood without involving varied A-site dopants.

2. Experimental

Single-phased $La_{0.6}Ca_{0.4}CoO_{3-x}$ powder was prepared by an amorphous citrate precursor method [1,11,12]. A solution containing a mixture of citric acid and constituent metal nitrates, including $La(NO_3)_3$, $Ca(NO_3)_2$, and $Co(NO_3)_3$, was gradually evaporated at 75 °C until a gel was formed. The molar ratio of citric acid to the metal nitrates was 1:1. The gel was then calcined at increasing temperatures up to 930 °C. The resulted powder was then further annealed in vacuum (800–900 °C; <0.01 Torr) for 1 h to create oxygen deficiency. Oxygenation was carried out by consecutively annealing the vacuum-treated powder in flowing synthetic air (N_2:$O_2 = 21$:79; 22% RH) at temperatures decreasing from 800 to 100 °C with a decrement ranging from 50 to 200 °C. After annealing for a holding time of 5 h at every selected temperature, part of the powder was removed for electrochemical and material characterizations and the rest was further annealed at lower temperatures. X-ray diffraction (XRD) was carried out on a Mac-Science/MXP diffractometer with Cu Kα radiation, while X-ray photoelectron spectroscopy was conducted with Mg Kα radiation (15 kV, 20 mA, $hv =$ 1253.6 eV). Nitrogen adsorption (ASAP2000, Micromeritics) was conducted to determine the BET surface area. Temperature-programmed reduction (TPR) analysis was carried out under a flowing gas mixture containing 10 mol% H_2 in nitrogen with a flowing rate of 30 ml/min and a linear heating rate of 10 °C/min.

To prepare the active layer of the air electrode, a mixture containing the oxide, carbon black (VULCAN® XC72, Cabot Corp., USA), and PTFE suspension (60 wt.% in H_2O; Aldrich Chemicals) with weight ratios of 6:3:1 were first mixed and ground in excess ethanol and then dried at 85 °C to give a dough-like paste, which was finally rolled into a thin layer of ~200 μm thickness. A diffusion layer containing only carbon black and PTFE was prepared by the same process. The active and diffusion layers were finally rolled together with a stainless steel mesh in between. The air electrode was characterized with a three-electrode configuration with a Pt counter-electrode and a Hg/HgO/OH^- (7 M) reference electrode. The electrolyte is 7 M KOH. The polarization curves were acquired on an electrochemical analyzer (Eco Chemie PGSTAT30) under a constant potential-sweep rate of 2 mV/s.

3. Results and discussion

XRD analysis (curve 1, Fig. 1) showed that the reflections of the powder calcined at 930 °C were consistent with the single-phase $La_{0.6}Ca_{0.4}CoO_{3-x}$ [13]. Following annealing in vacuum, while the powder retained about the same lattice structure, there was particularly noticed the appearance of CoO phase (curve 2, Fig. 1) as well as shrinkage in unit-cell parameters. The higher the vacuum-annealing temperature, up to 900 °C, the greater the amount of CoO produced. The results suggest that, when oxygen vacancies were created, the lattice structure was stabilized by leaching out Co cations, which are primarily at the divalent state. After oxygenation at 800 °C for 5 h, CoO disappeared (Fig. 2). The XRD patterns remained approximately the same after oxygenation at decreasing temperatures from 800 to 100 °C except for small variations in lattice parameters (Fig. 2). Both the a- and c-axes were found gradually shortened with increasing extent of oxygenation (Table 1), and the volume of unit-cell decreases accordingly (Table 1 and Fig. 3). It was also noticed that all the oxygenated powders have longer axes than the vacuum-treated one (Table 1).

As shown by nitrogen adsorption, the (BET) specific surface area of oxide powder, which is 9.7 m^2/g, showed essentially no change after the consecutive oxygenation processes. TPR analysis gave three reduction peaks at ~400, 600, and 650 °C, respectively (Fig. 4). Calculation calibrated against the TPR spectrum of Co_2O_3

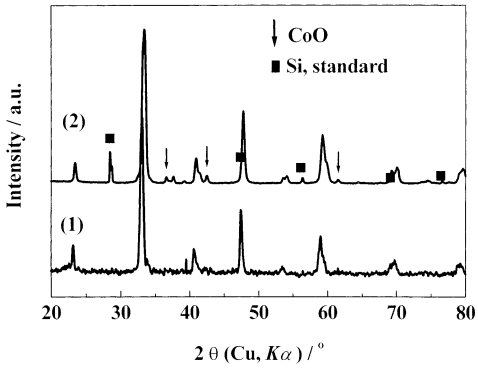

Fig. 1. Effect of vacuum annealing. Shown are XRD patterns for (1) single-phase $La_{0.6}Ca_{0.4}CoO_{3-x}$ synthesized in air and (2) the same powder annealed in vacuum (800 °C for 1 h). Note the appearance of CoO phase in (2).

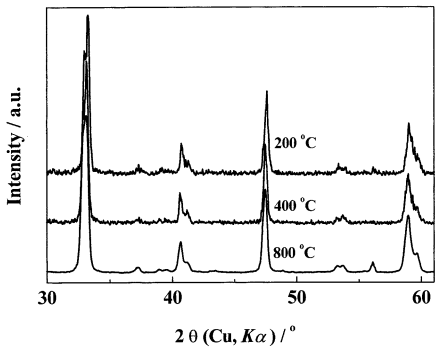

Fig. 2. XRD patterns for the powders after oxygenation. The temperatures indicated are those of the final oxygenation step. Note the shift of the reflections toward higher angle with decreasing oxygenation temperature due to shrinkage in lattice parameters.

Table 1
Lattice parameters of $La_{0.6}Ca_{0.4}CoO_{3-x}$ following different post-calcination annealing processes

Final annealing condition	Lattice parameters[a] (Å)		Unit-cell volume (Å^3)
	a	*c*	*V*
800 °C in vacuum	5.401	13.063	329.96
800 °C in air	5.437	13.205	338.03
600 °C in air	5.450	13.126	337.64
400 °C in air	5.449	13.125	337.47
300 °C in air	5.436	13.110	335.54
200 °C in air	5.436	13.072	334.54
100 °C in air	5.413	13.095	332.22

[a] The lattice parameters have been calculated according to hexagonal axes as listed in ICDD Card No. 36-1389 [13].

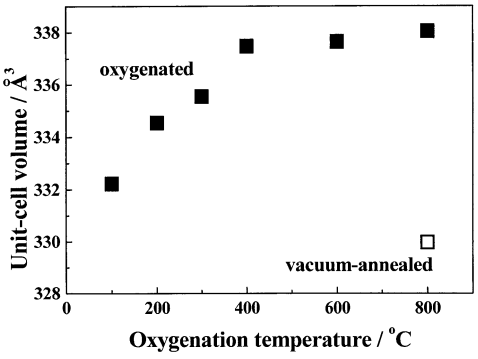

Fig. 3. Unit-cell volume versus the temperature of the final annealing step. Datum of the vacuum-annealed powder (open symbol) is also shown.

indicated that the integrated intensities of the entire spectra (up to 750 °C) of the oxygenated powders corresponded to the reduction of a valence close to 3, and the ratio between the intensity of the first peak (up to 480 °C) and that of the last two overlapped peaks (between 480 and 750 °C) was in the order of 1:2. Furthermore, XRD analysis of the reduced powder

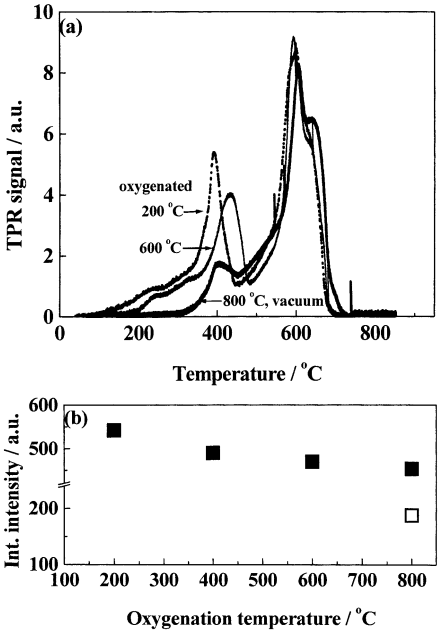

Fig. 4. (a) Temperature-programmed reduction (TPR) spectra. The temperatures indicated are those of the final oxygenation step. (b) The integrated intensity (up to 480 °C) as a function of the final oxygenation temperature. Datum of the vacuum-annealed powder (open symbol) is also shown.

quenched from 800 °C showed the presence of La_2O_3, CaO, and Co (Fm3m). It is thus concluded that the observed reduction events are due to consecutive reduction of Co cation from +3 to +2 for the 400 °C-peak and then to the zero-valence state for the 600 and 650 °C-peaks, respectively. Furthermore, the reduction temperatures are higher than those observed for Co_2O_3 (250–400 °C), suggesting that the Co cations were mostly not in the elemental oxide state during the course of reduction. Powders subjected to different extents of oxygenation showed significant variations primarily in the peak temperature and intensity associated with reduction of Co^{3+} (i.e., the 400 °C-peak). The peak temperature decreases (Fig. 4a), while the peak intensity increases (Fig. 4b), suggesting increasing amount of Co^{3+}, with consecutive oxygenation at lower temperatures. Once Co^{3+} was reduced to Co^{2+}, all powders gave about the same intensities for the subsequent two reduction events.

The results from both XRD and TPR analyses, which characterized mainly the bulk properties of the powders, indicated that the oxygen content of the oxide indeed increased after consecutive oxygenation at descending temperatures. The gradual shortening in lattice axes upon oxygenation is a natural result from increasing total number of bonds between cations and oxygen anions as oxygen vacancy is gradually filled. Furthermore, the TPR results revealed that the valence of Co

cation, changing from +2 to +3, is susceptible to oxygenation.

Fig. 5a and b show, respectively, the anodic and cathodic polarization curves for the electrodes comprising the oxide catalyst subjected to different post-calcination treatments, while Fig. 6a and b summarize the currents at fixed potentials as a function of oxygenation temperature. The catalytic activities indeed showed strong dependence on the post-calcination thermal protocol, and the Faradaic currents showed more than fourfold variation upon different vacuum and oxygenation processes. The vacuum-annealed powder has the lowest catalytic activity. Upon oxygenation, both the cathodic and anodic currents first monotonically decrease with consecutive oxygenation at lower temperatures till 300 °C (Fig. 6). The currents then rise rather abruptly with the rate of oxygen evolution (the anodic current) reaching the maximum at 150 °C and that of reduction (the cathodic current) at 200 °C.

Bockris and Otagawa [2], in their study on electrocatalytic activities of several $LaMO_3$ perovskite oxides for oxygen evolution, where M is a transition metal, suggested that the reaction site for oxygen evolution is at the M-ion, i.e., the B-site cation, and that the evolution rate is determined by the bonding strength between the B-site cation and OH^- group on the catalyst surface. They pointed out a correlation showing increasing electrocatalytic activity of the oxide with decreasing

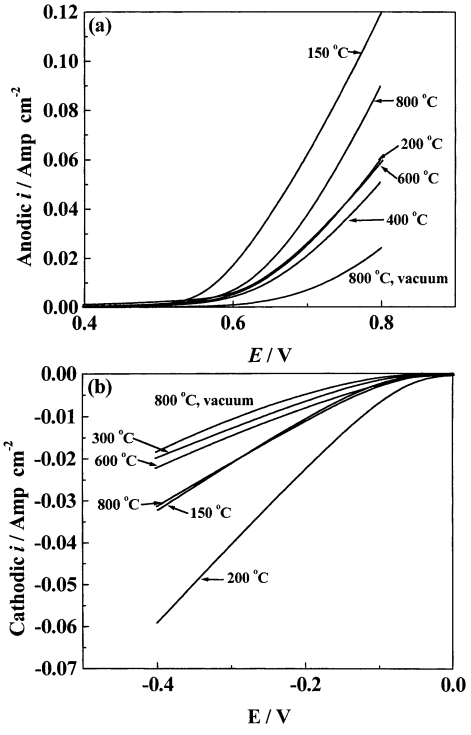

Fig. 5. Anodic (a) and cathodic (b) polarization curves for the electrodes comprising the oxide catalysts subjected to oxygenation at different temperatures. Curves of the vacuum-annealed powder are also shown.

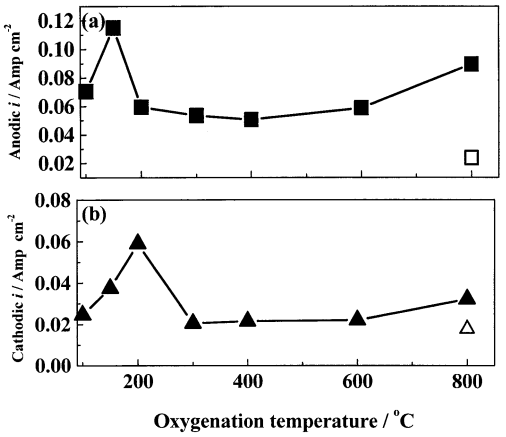

Fig. 6. Currents at fixed potentials (−0.4 and 0.8 V versus Hg/HgO/OH^- (7 M) for cathodic and anodic polarization, respectively) as a function of the final oxygenation temperature. Data of the vacuum-annealed powder (open symbols) are also shown.

average oxygen bonding strength in the lattice and indicated that these two bonding strengths were related. This view of the B-cation reaction site explained several observations in this study. First, vacuum annealing caused leaching out of Co cations for balancing oxygen vacancies, resulting in a decrease in the number of reaction active site, i.e., the Co-ion site. As a result, the freshly vacuum-annealed powder has the lowest electrocatalytic activity. Secondly, the decreasing unit-cell volume with increasing oxygen content (Fig. 3) indicated stronger bonding among metal cations and oxygen anions. In addition, TPR analysis also indicated that Co cation in general became increasingly positive-charged upon oxygenation. Both results pointed to the expectation of a greater Co–OH bonding strength, and hence account for the decreasing trend in activity with consecutive oxygenation at lower temperatures. Our observations are also in accordance with those of Lee et al. [3], who reported that fast cooling at the end of synthesis of $La_{0.6}Ca_{0.4}CoO_{3-x}$ powder resulted in a higher activity than slow cooling.

The increases in catalytic activities after prolonged oxygenation below 300 °C are, however, rather unexpected, as neither TPR nor XRD data exhibit any adverse change in bulk properties. On the other hand, these enhancements may be caused by the significant changes in surface chemistry/structure as indicated by XPS analysis. It was found that both O 1s and La 3d XPS spectra exhibited doublets for all powders (Figs. 7 and 8). The same results were also observed on single-phase La_2O_3 powder. The doublets of the O peak can be attributed to surface OH and lattice O (Fig. 8a), respectively, while the doublets of the La peak may indicate mainly two types of bonding configuration between La cations and these oxy species at surface. The OH species must have been formed during, but not after, thermal treatment, as the length of storage at

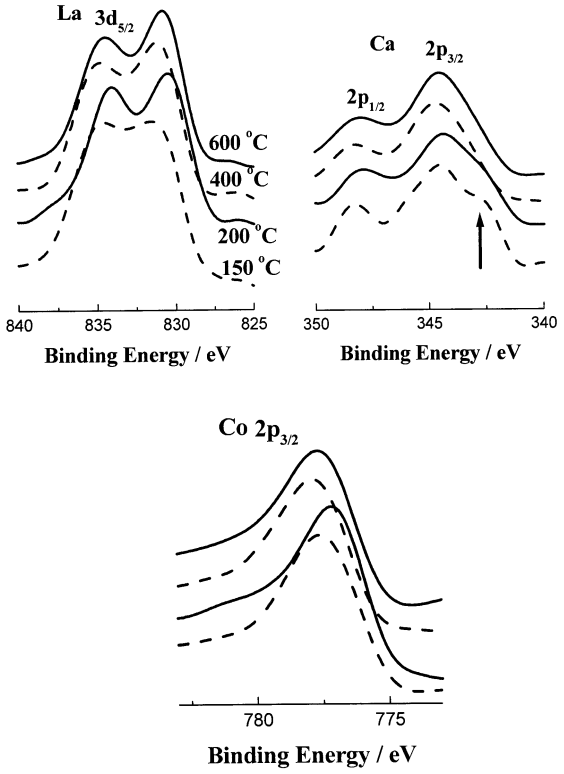

Fig. 7. XPS spectra of La $3d_{5/2}$, Ca $3p_{3/2}$, and Co $2p_{3/2}$. The temperatures indicated are those of the final oxygenation step.

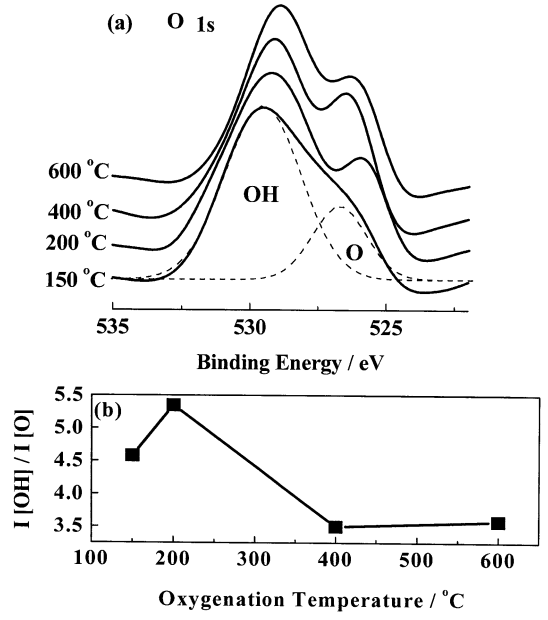

Fig. 8. (a) O 1s XPS spectra. The temperatures indicated are those of the final oxygenation step. (b) The intensity ratio between the OH and lattice O peaks de-convoluted as indicated in (a) as a function of the final oxygenation temperature.

room temperature does not affect the spectrum intensity. No doublet was observed for the spectrum of either O or cation in the cases of Co_3O_4 and CaO, suggesting that Co and Ca cations have a much lower affinity toward hydroxyl than La. By de-convoluting the O 1s doublets, the intensity ratio between the OH and lattice O peaks, I[OH]/I[O], was calculated, and there observed a significant increase in the ratio for oxygenation below 200 °C (Fig. 8b). Concurrently, Co $2p_{3/2}$ peak shifted toward lower binding energy (BE; Fig. 7). The larger the ratio, the greater the shift. The increased OH coverage may be associated with Co cations. In addition, there was noticed a shoulder for the Ca $2p_{3/2}$ peak toward the lower BE end (arrow, Fig. 7), which emerged after oxygenation at 200 °C and became manifest at 150 °C. It indicated the occurrence of a type of less charged surface Ca cations.

By referring to the CV data (Fig. 6), there is clearly a good correlation between the rise in cathodic current and the increase in I[OH]/I[O] ratio. The maximum anodic current, on the other hand, appears to coincide with the occurrence of the less charged Ca cations, but the correlation is less clear. Even though the detailed structures of the surface species and their relations with the catalytic activities of the oxide have yet to be determined, the results clearly point out what a profound effect a thermal treatment at temperatures even below 300 °C could have on the surface structure, and hence on the catalytic properties of the oxide.

In summary, upon being consecutively annealed at temperatures descending from 800 to 100 °C, the catalytic activities of $La_{0.6}Ca_{0.4}CoO_{3-x}$ toward oxygen reduction and evolution were found affected by two mechanisms. Annealing above 300 °C results in an increase in oxygen content and concurrently a decrease in the activities. On the other hand, annealing below 300 °C leads to maximum activities, which likely result from changes in the surface chemistry/structure.

References

[1] Y. Shimizu, K. Uemura, H. Mtsuda, N. Miura, N. Yamazoe, J. Electrochem. Soc. 137 (1990) 3430.
[2] J.O'M. Bockris, T. Otagawa, J. Electrochem. Soc. 131 (1984) 290.
[3] C.K. Lee, K.A. Striebel, F.R. McLarnon, E.J. Cairns, J. Electrochem. Soc. 144 (1997) 3801.
[4] M.S.G. Baythoun, F.R. Sale, J. Mater. Sci. 17 (1982) 2757.
[5] S. Muller, K. Stiebel, O. Haas, Electrochim. Acta 39 (1994) 1661.
[6] S. Muller, O. Haas, C. Schlatter, Ch. Comninellis, J. Appl. Electrochem. 28 (1998) 305.
[7] U. Geiser, M.A. Beno, A.J. Schultz, H.H. Wang, T.J. Allen, M.R. Monaghan, J.M. Williams, Phys. Rev. B 35 (1987) 6721.
[8] G.P. Luo, Y.S. Wang, S.Y. Chen, A.K. Heilman, C.L. Chen, C.W. Chu, Y. Liou, N.B. Meng, Appl. Phys. Lett. 76 (2000) 1908.
[9] H. Takang, S. Uchida, K. Kitazawa, S. Tanaka, Jpn. J. Appl. Phys. 26 (1987) L218.
[10] S.K. Tiwari, S.P. Singh, R.N. Singh, J. Electrochem. Soc. 143 (1996) 1505.
[11] M.S.G. Baythoun, F.R. Sale, J. Mater. Sci. 17 (1982) 2757.
[12] H.M. Zhang, Y. Teraoka, N. Yamazoe, Chem. Lett. (1987) 665.
[13] International Center for Diffraction Data (ICDD), Newtown, PA, File Card No. 36-1389.